Pure and Applied Geophysics

Correlation Between Local Slip Rate and Local High-frequency Seismic Radiation in an Earthquake Fault

ALEXANDER A. GUSEV,[1,2] EUGENIA M. GUSEVA,[2] and GIULIANO F. PANZA[3,4]

Abstract—For any earthquake, the slipping fault and the source of high-frequency seismic waves, by and large, coincide. On a more local scale, however, the areas of high seismic slip rate and of increased high-frequency radiation output (seismic luminosity) need not match. To study in some detail how slip rate and seismic luminosity are interrelated, a systematic study is performed that uses 251 records of teleseismic P waves from 23 intermediate-depth earthquakes of magnitude 6.8 and above. From a broadband trace we extract two time histories: (1) displacement and (2) 0.5–2.5 Hz band-passed and squared velocity, or "HF power", and calculate correlation coefficient, ρ between the two. To reduce the bias related to formation of P coda, a special procedure is applied to data. We estimated the average value $\rho = 0.52$ (range of event averages 0.35 to 0.65) for the correlation coefficient between the radiated time histories for displacement and "HF power", which is considerably below the "ideal" value of unity. We argue that the same or even lower value characterizes the degree of slip rate - seismic luminosity correlation at the fault. Two factors may contribute to the revealed decorrelation: (1) random fluctuations of observed HF power (inevitable for a signal with a limited bandwidth), and (2) the genuine mismatch of slip rate and mean luminosity. We show that these factors, acting separately, would result in the ρ values equal to, correspondingly, 0.72 and 0.80. We also show that genuine decorrelation is statistically significant. We conclude that the observed values of ρ indicate genuine differences between the distributions of the slip rate and the seismic luminosity over the fault area. These results provide important constraints both for the accurate wide-band simulation of strong ground motion and for theoretical dynamic source models.

Key words: Earthquake fault, stochastic, high-frequency radiation, envelope, seismic energy, non-coherent, strong motion simulation.

Introduction

It is widely accepted that the source of seismic waves, including high-frequency (HF) waves, is a fast-slipping patch on a geological fault, named earthquake fault.

[1] Institute of Volcanology and Seismology, Russian Ac. Sci., 9 Piip Blvd., Petropavlovsk-Kamchatsky, 683006, Russia. E-mail: gusev@emsd.iks.ru
[2] Kamchatka Branch, Geophysical Service, Russian Ac. Sci., 9 Piip Blvd., Petropavlovsk-Kamchatsky, 683006, Russia
[3] Department of Earth Sciences, University of Trieste, Via E. Weiss 4, 34127, Trieste, Italy
[4] The Abdus Salam International Centre for Theoretical Physics, SAND Group, Trieste, Italy

This means that HF seismic energy is generated only while a particular patch of the fault is slipping. However, the majority of fault models that deal with HF radiation presuppose much more than that. Usually it is assumed that the HF radiation increases with increasing slip rate, or, for composite models, that HF energy from a subsource increases with the increase of its seismic moment. Examples are composite models formulated by BLANDFORD (1975), HANKS (1979), BOATWRIGHT (1982; 1988), PAPAGEORGIOU and AKI (1983), and GUSEV (1989). This assumption is no more than an initial approximation. To find out how close, in real earthquakes, it is the actual correlation between slip rate and HF radiation output, an independent inversion for each of the two quantities that is needed. For brevity, henceforth, we shall call the HF radiation output, or more accurately the radiated HF power per unit source area, "seismic luminosity" or, merely, "luminosity", transferring to seismology the standard light-engineering term for the similar parameter used to specify the radiated light power.

At present, a considerable number of inversions for space-time distributions of luminosity (or its time integral) have been performed (IIDA and HAKUNO, 1984; GUSEV and PAVLOV, 1991, 1998; ZENG *et al.*, 1993; KAKEHI and IRIKURA, 1996; NISHIMURA *et al.*, 1996, PETUKHIN *et al.*, 2004). These inversions show that the spatial distributions of luminosity may resemble those of the slip rate, although significant differences can often be seen. Therefore observations do not indicate any tight slip rate-luminosity relationship.

The inversion of the slip rate and luminosity in space-time can be made only with individual earthquakes, and has a limited resolution. In the following we try to extract information on the correlation between slip rate and luminosity directly from body-wave records. With this purpose we analyze the correlation between time histories of far-field displacement and far-field HF squared velocity, or HF power. We believe that this correlation reflects, to a large degree, the correlation between source slip rate and source luminosity. In particular, low correlation between displacement and HF power signals indicates low slip rate-luminosity correlation in the source.

Empirically we find significant slip rate-luminosity decorrelation. This fact can have two radically different causes: "fluctuational" decorrelation, or a simple effect of statistical fluctuations of HF signal power, or "physical" decorrelation—a genuine difference between space-time distributions of slip rate and of luminosity. We shall endeavor to separate these two effects, and to demonstrate that a significant contribution of genuine decorrelation is present in data.

When one tries to analyze the correlation between displacement and HF power signals, one meets with a problem: the HF signal is markedly distorted by scattering along the path; this is seen most prominently in the formation of *P* coda. To overcome this obstacle, before comparing displacement and HF power signal, we artificially distort the displacement signal by convolution with the "HF power Green's function" of the medium.

The plan of the work is as follows. (1) A simplified theoretical background to our data analysis is presented. (2) We examine teleseismic P waves from large intermediate-depth earthquakes, select data of acceptable quality, and choose a common HF band to extract HF power signal. Then, displacement and HF power signals are calculated. (3) We determine an appropriate envelope function that emulates the formation of P coda and convolve it with displacement signals. (4) We calculate correlation coefficients between modified displacement and HF power time histories. (5) We determine the expected value for the same correlation coefficient for the ideal case of "purely fluctuational" decorrelation, and compare it with empirical correlations. We find that the latter are significantly lower, thus indicating the reality of "physical" decorrelation.

Theoreical Background for Data Analysis

Basic Assumptions

A few basic assumptions are to be mentioned to substantiate our analysis. Initially we specify what high-frequency (HF) signal is. We shall always assume in the following that the received seismic body wave signal is band-pass filtered, with central frequency f_0 of the band considerably larger (practically, 5–10 times and more) than the corner frequency f_c of the body wave displacement ($f_c \approx 1/T$, where T is the source process duration), and with bandwidth Δf. Our main conceptual assumption is that the HF radiation from an earthquake fault is non-coherent. This means that we can ignore phase spectra of signals (treating them as random), and therefore assume additivity of signal power instead of the usual additivity of signal amplitudes. In particular, we believe that the fault can be assumed to consist of a large number of spots whose contributions of HF energy into wave intensity at the receiver are additive. To warrant additivity, HF fault motion over different spots is assumed statistically independent.

Some assumptions regarding non-coherency are inevitable if one plans to treat an earthquake source in a stochastic manner, and our assumptions are most primitive. Of course, the adequacy of such an approach cannot be proved in any strict sense, and only the practically reasonable results can warrant it. Note that the hypothesis of incoherency is actually very widely accepted. In particular, it is the basis for wide-band fault representation by multiple random subsources (e.g., HANKS, 1979; PAPAGEORGIOU and AKI, 1983) that is essentially a standard in modern practical simulation of finite faults. It is also a standard assumption in inversions of HF radiation from earthquake faults (GUSEV and PAVLOV, 1991; ZENG et al., 1993; KAKEHI and IRIKURA, 1996; NISHIMURA et al., 1996 and later work). Coherency at high frequencies means, essentially, a kind of deterministic behavior; it may be noted in this relation that all deterministic fault models predict completely unrealistic HF signal.

The uncorrelated contributions from fault spots are added at the receiver with various delays to produce a random-like HF record. Therefore, the main variable below will be squared band-passed particle velocity $\dot{u}^2(t)$ at the receiver. To be accurate, we should distinguish between: (1) an ideal notion of mean squared velocity ($\langle\dot{u}^2(t)\rangle$), that specifies the statistical ensemble, and (2) its empirical estimate from a single observed realization – average squared velocity ($\overline{\dot{u}^2(t)}$). When multiplied by $c\rho$ (c: wave speed, ρ: density) both give true wave intensity (W/m²), ideal or empirical. For clarity, we shall call this signal further as HF power signal.

This description is in fact oversimplified. An HF body-wave seismogram reflects not only the source space-time function but also the actual medium response produced by scattering (here we use the term "scattering" loosely to cover both scattered and converted waves). Both (source and medium) components can be treated as random signals and be specified by their mean square amplitudes. Fortunately, for non-coherent signals we can assume that the effect of scattering can be represented by convolution of source signal and "HF power Green's function" (HFPGF), that represents the non-coherent response of the medium to a delta-like input (Ishimaru 1978). On such a basis, Gusev and Pavlov (1991, 1998) reconstructed the source HF power signal by deconvolution, using the record of an aftershock as an HFPGF. In the following, we shall employ this convolution concept, although in a different way. Namely, before analyzing correlation between HF power signal and low-frequency displacement signal, we shall distort the displacement signal by convolution with a typical medium response.

Let us consider the relation between luminosity of a non-coherent body-wave radiator and HF power signal , or radiation intensity, at a receiver, for a chosen frequency band Δf. Let Σ be the flat surface of the radiator, with element dS whose location is defined by coordinate vector $\boldsymbol{x}$. Let us introduce scalar luminosity function $L(\boldsymbol{x},t)$ of a radiator for the same frequency band, so that $L(\boldsymbol{x},t)dS$ is the mean wave power flux from dS at a time t. In the far-field case considered here, the radiation pattern is the same for any dS. In homogeneous medium, assuming additivity, the energy at a receiver at $\boldsymbol{y}$ is

$$c\rho\langle\dot{u}^2(t+R/c)\rangle = \langle W(\boldsymbol{y},t+R/c)\rangle = A^2(\boldsymbol{m},\boldsymbol{r},R)\int_\Sigma L(\boldsymbol{x},t+\boldsymbol{x}\cdot\boldsymbol{r}/c)\,dS, \qquad (1)$$

where $R = |\boldsymbol{y}|$, $\boldsymbol{r} = \boldsymbol{y}/|\boldsymbol{y}|$, c is wave velocity, $\boldsymbol{m}$ is unit seismic moment tensor at Σ, and $A^2(\boldsymbol{m},r,R)$ describes the effects of geometric spreading and radiation pattern, common for all points of a fault. The case of a scattering medium can be represented in a similar, though a slightly more cumbersome, way and does not introduce significant complications.

Unfortunately, Equation (1) is mostly of symbolic value because dS cannot be infinitesimally small. In a more rigorous treatment, instead of integral, one should consider a finite sum over statistically independent spots of area ΔS_i,

$$\langle W(\boldsymbol{y}, t + R/c) \rangle \approx A^2(m, \boldsymbol{r}, R) \sum_i L_i(\boldsymbol{x}_i, t + \boldsymbol{x}_i \cdot \boldsymbol{r}/c) \Delta S_i, \tag{2}$$

where i enumerates these spots, and $\boldsymbol{x}_i$ is the center or centroid of i-th spot. Representation of $L(\boldsymbol{x}, t)$ through the fault slip is not straightforward (see (GUSEV, 1983) for incomplete solution); this derivation shall be given elsewhere. Here we confine ourselves to several notes. The most important point is that the spot size ΔS_i, is not arbitrary, but must be close to $\pi R_c{}^2$ (GUSEV, 1983) where R_c is the correlation distance of a source (for the given f_0). For a "perfectly non-coherent" random source one can expect that the diameter $2R_c$ of a "coherent" spot (whose points move in a coordinated fashion), is near the wavelength $\lambda = c/f_0$. As for the correlation time T_c of filtered local fault motion, we expect it to be equal to $1/\Delta f_0$, as usual for band-limited noises. In an important case of an octave bandwidth and "a perfectly non-coherent" source, $T_c = 1.4 R_c/c$. Therefore, the values of source slip rate function at space-time points $(\boldsymbol{x}, t)$ and $(\boldsymbol{x}', t')$ are assumed uncorrelated if $|\boldsymbol{x} - \boldsymbol{x}'| \gg R_c$ or $|t - t'| \gg T_c$, and tightly correlated in the cases of opposite inequality. The more general case of imperfect incoherence (with larger space-time volumes of correlated motion) will not be treated here.

To analyze the correlation between fault slip rate and fault luminosity, we assume that $R_c \ll L$ and $T_c \ll T$, where L and T are source length and duration. Then on the basis of the usual integral

$$u(\boldsymbol{y}, t + R/c) = A(m, \boldsymbol{r}, R) \int_\Sigma \dot{D}(\boldsymbol{x}, t + \boldsymbol{x} \cdot \boldsymbol{r}/c) \, dS \tag{3}$$

that relates fault slip rate $\dot{D}(\boldsymbol{x}, t)$ and far-field displacement $u(\boldsymbol{y}, t + R/c)$, we can write an integral sum and assume that approximately

$$u(\boldsymbol{y}, t + R/c) \approx A(m, \boldsymbol{r}, R) \sum_i \dot{D}_i(\boldsymbol{x}_i, t + \boldsymbol{x}_i \cdot \boldsymbol{r}/c) \Delta S_i. \tag{4}$$

We would like to compare similar equations (2) and (4). Specifically, we are interested here in how a possible correlation between $\dot{D}(\boldsymbol{x}, t)$ and $L(\boldsymbol{x}, t)$ shall be manifested in correlation between $W(\boldsymbol{y}, t)$ and $u(\boldsymbol{y}, t)$ at the same $\boldsymbol{y}$, or at the same receiver. In the following we shall consider a particular receiver, and drop the $\boldsymbol{y}$ argument. We also discretize the time scale ($t \rightarrow t_k$) using the time step about T_c so that successive counts of $L_i(\boldsymbol{x}, t)$ are approximately independent. Also redenote $\dot{D}_i(\boldsymbol{x}, t_k)$ as $S_{ik} = S_m$, where $m = (i, k)$ is multiindex that enumerates all coherent spots and all time samples; similarly introduce $L_m = L_{ik} = L_i(\boldsymbol{x}, t_k)$. Let us consider covariance between S_m and L_m (at a certain m). Let us also assume that the correlation properties of the fault process are stable in space and time, so that the correlation coefficient is identical ($= \rho_1$) for different m:

$$\mathrm{Cov}(S_m, L_m) = \sigma(S_m)\sigma(L_m)\rho_1, \tag{5}$$

where $\sigma(S_m) = \mathrm{Var}^{0.5}(S_m)$, $\sigma(L_m) = \mathrm{Var}^{0.5}(L_m)$. For discretized u and W signals at time sample number n, one can write

$$u_n = A\sum_m B_{nm}S_m; \quad W_n = A^2\sum_m B_{nm}L_m, \tag{6}$$

where B_{nm} is matrix representing the delay-and-sum operation in (2) and (4). Now one can write

$$\mathrm{Cov}(u_n, W_n) = \mathrm{E}(u_n W_n) = A^3 \sum_m \sum_p B_{nm}B_{np}\mathrm{E}(S_m L_p). \tag{7}$$

First consider the special case when luminosity at a spot i and time sample k is correlated only with slip rate at the same $(i,k) = m$. Then there is zero correlation between S_m and L_p at $m \neq$ p, and the double sum in (7) reduces to a single sum, giving, through (5):

$$\mathrm{Cov}(u_n, W_n) = A^3 \sum_m B_{nm}^2 \sigma(S_m)\sigma(L_m)\rho_1 = \sigma(u_n)\sigma(W_n)\rho_1. \tag{8}$$

In more general cases, cross terms shall appear in the double sum. Generally speaking, they can be either positive or negative. From a physical point of view, positive correlation means that for a pair of spots or for a pair of time segments, an increase of slip rate in one of them is accompanied by an increase of luminosity in another. This is quite possible if a significant part of a fault moves (or radiates HF energy) in a coordinated fashion. (With respect to slip rate in particular, such coordinated motion is in accordance with the AKI's (1967) ω^{-2} time history spectrum and ANDREWS' (1980) proposal of k^{-2} spectrum of final slip.). In such a case, a significant positive correlation of luminosity with slip on a certain spot shall be accompanied by similar, though smaller, positive correlation with slip on adjacent spots. It is considerably more difficult to imagine causes of negative correlation, and we shall consider the contribution of such pairs as limited and certainly overweighed by terms with positive correlation. Therefore, there is a good probability that double sum (7) shall be larger or equal to its "diagonal version" (8), so that in general

$$\mathrm{Cov}(u_n, W_n) = \sigma(u_n)\sigma(W_n)\rho_2 \tag{9}$$

with $\rho_2 \geq \rho_1$ Hence, the correlation coefficient between displacement and HF power signals in the wavefield either reproduces, or gives an overestimate of the correlation coefficient between fault slip rate and fault luminosity.

    This derivation assumed delta-like Green function of body wave (represented by the time delay R/c and by factor A). For more complex media, effects of multipathing and/or random scattering can be represented as a linear operator, and in discretized form its introduction shall only modify the **B** matrix. Our derivation is independent of a particular form of this matrix, and thus holds true also for this

more general case. Similarly, linear data processing, including smoothing, shall not modify this result.

To apply these important results to data analysis, we would need, formally, multiple realizations of a single source that produce multiple $[u(t), W(t)]$ pairs *for a given t*. As is often done in geophysics, we shall assume ergodicity, and perform averaging over a set of u-W sample pairs extracted from a single pair of observed $[u(t), W(t)]$ functions at *different times t*. In this manner we can obtain a consistent estimate of the covariance and thus correlation coefficient. In this estimation, the input data should be sampled with a certain step, of about $1/\Delta f_0$. More frequent sampling is redundant. Furthermore, to stabilize results, it is useful to smooth $W(t)$ and then to apply more rarified sampling; of course, similar smoothing must be applied to $u(t)$. As a result, we shall obtain the empirical estimate for the correlation coefficient between sample functions $W(t)$ and $u(t)$, and this coefficient shall give us the upper bound for the similar coefficient between slip rate and average luminosity.

Luminosity-slip rate correlation: effects of fluctuating signal

The described approach can give us an estimation of empirical, observed correlations. It is interesting to derive similar estimates for ensemble averages, or means (the "ideal case"). The interest in the "ideal" values is not purely academic. When the stochastic approach is used for simulations of strong motion, it is *mean* square amplitude for fault motion that one must adequately specify, in order to obtain realistic example motions over the fault and at a receiver. The difference between the estimates for a realization and the mean value is caused by the fact that with observed data, we are estimating correlation coefficient using a fluctuating signal. These fluctuations are caused by inevitable oscillations of amplitude of a band-limited signal, that take place even when mean signal power is strictly constant. Fluctuations introduce decorrelation, and the empirical estimate of correlation shall be lower than its "ideal" value. To clarify how additional decorrelation appears because of fluctuations, consider a model case of two copies/realizations of a segment of quasi-stationary band-limited noise, with slowly-varying mean power. In this case, the "ideal" correlation coefficient between *mean* squared amplitudes equals to unity by construction; whereas for any actual pair of *realizations*, this coefficient, obtained from two independent sets of squared noise amplitudes, will always be less than unity. (It approaches unity as the bandwidth increases infinitely; however this fact is useless for seismological application).

Now we introduce denotations: ρ_{ob} is the "observed" correlation coefficient ($= \mathrm{Corr}(W(t), u(t))$), and ρ_{id} is the "ideal" (ensemble mean) correlation coefficient ($= \mathrm{Corr}(\langle W(t) \rangle, u(t))$). It is the latter that, in frames of the stochastic approach, describes the intrinsic mechanism of data generation. Consider first the hypothetic

"perfect-correlation" case when Corr $(\langle W(t)\rangle, u(t)) = \rho_{id} = 1$. In this case, decorrelation is minimal and produced by fluctuations only. For each particular pair of realizations $[W(t), u(t)]$, we then have a particular value of correlation coefficient that we denote ρ_{idpr} (for "ideal", "perfect", "in realization"). This parameter ρ_{idpr} is a random variable, fluctuating from realization to realization. Is important to know the statistical distribution of these fluctuations: with this distribution at hand, we can test statistically the hypothesis $\rho_{id} < 1$ on the basis of the given value of ρ_{ob}. Assuming normal distribution for ρ_{idpr}, we need to know mean $E(\rho_{idpr})$ and standard deviation $\sigma(\rho_{idpr})$. Note that $E(\rho_{idpr})$ is not equal to ρ_{id}: when ρ_{id} is around 0.5–1, $E(\rho_{idpr})$ is always smaller than ρ_{id}. To determine $E(\rho_{idpr})$ and $\sigma(\rho_{idpr})$ in a real situation, we can use Monte-Carlo approach. We take the observed long-period signal $u(t)$ and use it as a mean envelope function for a "perfect-correlation" HF power signal $W^*(t)$. Using this prescribed envelope, we simulate a number of realizations (say, 25) of band-passed modulated noise (each of them appears like $\dot{u}(t)$). From these 25 artificial data we estimate $E(\rho_{idpr})$ and $\sigma(\rho_{idpr})$.

With ρ_{ob} and $E(\rho_{idpr})$ values at hand, we might estimate the ρ_{id} value that underpins our data, provided we can establish a theoretical relationship among ρ_{ob}, $E(\rho_{idpr})$ and ρ_{id}. In order to find such a relationship we shall construct a simple model of a fluctuating signal. Let us consider a random vector $\boldsymbol{a} = \{a_i\}$ whose components describe the sequences of (positive) amplitudes of $u(t)$; the components a_i have the same distribution and they can be mutually correlated in some irrelevant way. To represent the different degrees of correlation between $u(t)$ and $W(t)$ we introduce another vector $\boldsymbol{b}$, with the same properties as $\boldsymbol{a}$ but statistically independent from $\boldsymbol{a}$, and form the vector $\boldsymbol{d}_0$, that represents $\langle W(t)\rangle$, and defined as:

$$\boldsymbol{d}_0 = p\boldsymbol{a} + (1-p)\boldsymbol{b} = p\boldsymbol{a} + q\boldsymbol{b}, \tag{10}$$

where p is the degree of correlation ($0 < p < 1$) and $q = 1-p$. It is easy to show that the correlation coefficient between $\boldsymbol{a}$ and $\boldsymbol{d}_0$ is

$$\rho_{id} = \mathrm{Corr}(\boldsymbol{a}, \boldsymbol{d}_0) = p(p^2 + q^2)^{-0.5}. \tag{11}$$

To imitate random fluctuations of $W(t)$ around its mean $\langle W(t)\rangle$, represent $W(t)$ as

$$\boldsymbol{d} = \boldsymbol{d}_0(1 + k\boldsymbol{s}), \tag{12}$$

where $\boldsymbol{s}$ is a random vector of the same size as $\boldsymbol{a}$, with zero mean, and the degree of fluctuations are defined by "distortion" coefficient $k > 0$. We further assume that $\boldsymbol{a}$ and $\boldsymbol{b}$ are distributed exponentially; this is accurate for the squared amplitude of the analytical signal formed from Gaussian noise, and such a representation is adequate for our aims. In general

$$\langle \rho_{ob}\rangle = \mathrm{Corr}(\boldsymbol{a}, \boldsymbol{d}) = p\left\{(p^2 + q^2) + k^2\mathrm{Var}(\boldsymbol{s})[p^2 + q^2 + \langle \boldsymbol{a}\rangle^2/\mathrm{Var}(\boldsymbol{a})]\right\}^{-0.5} \tag{13}$$

and in our special case of exponential law

$$\langle \rho_{ob} \rangle = \mathrm{Corr}(\boldsymbol{a}, \boldsymbol{d}) = p\left[p^2 + q^2 + z(p^2 + q^2 + 1)\right]^{-0.5}, \tag{14}$$

where we denoted z the unknown combination $k^2/\mathrm{var}(s)$. We shall use Equation (14) twice in succession. First, we find z: we set $p = 1$, $q = 0$, substitute $\langle \rho_{ob} \rangle$ by known $\mathrm{E}(\rho_{idpr})$, and solve the resulting equation with respect to z. Second, we estimate p: with known z at hand, we substitute $\langle \rho_{ob} \rangle$ by its empirical estimate ρ_{ob}, and derive the unknown p value. From p, the value of ρ_{id} is found through (11).

Compensating for Scattering of HF Waves

As we noted above, the additivity of power permits us to represent the HF power at the receiver as convolution:

$$W_s(\cdot) = W_o(\cdot) * W_h(\cdot), \tag{15}$$

where $W_s(t)$, $W_o(t)$ and $W_h(t)$ are the time histories for, respectively: HF power signal at a station; HF power signal at the source for the particular ray directed to the station, and for the HFPGF. In principle, one can try to recover $W_o(t)$ from $W_s(t)$ by applying inverse filtering (GUSEV and PAVLOV, 1991); but this procedure is too noisy for our aims. Instead, to obtain comparable low- and high-frequency signals, we decided to artificially distort the low-frequency signal by convolution with an operator that imitates $W_h(t)$. Then we can determine the correlation between comparable objects: (1) artificially distorted low-frequency signal $u^*(\cdot) = u(\cdot) * W_h(\cdot)$, further labeled "modified displacement" signal and (2) naturally distorted raw high-frequency signal $W_s(\cdot) = W_o(\cdot) * W_h(\cdot)$. As was noted above, this convolution should not decrease the value of the correlation coefficient (i.e., $\mathrm{Corr}(W_o(t), u(t)) \geq \mathrm{Corr}(W_s(t), u^*(t))$).

Data Set and Its Processing

To compare observed far-field displacement and HF power time functions, we need clear isolated body-wave signals with sufficiently high signal-to-noise (S/N) ratio over a sufficiently wide frequency band. These requirements led to the narrow magnitude range 6.8–7.6 for our data. From each "raw" teleseismic BB record we reconstruct the time histories for displacement and for squared HF band-filtered velocity, or HF power. These time histories are then used to analyze displacement-HF power correlation. An important practical step is the selection of signals with clear, one-sided (positive or negative) displacement time history. This type of signal is theoretically predicted for a planar shear source. Intermediate-depth earthquake sources mostly follow this model. Initially we selected all (31) earthquakes in the IRIS DMS database since 1990 with $M_w \geq 6.8$ and focal depth $H = 90–200$ km.

P-wave groups on broad-band vertical (BHZ) channels (sampling interval Δt_0 = 0.05 s) of GDSN stations at epicentral distances from 25° to 100° have been retrieved through the IRIS DMS center. We needed records with no overlapping of *P*- and *pP*-wave groups, and those with one-sided displacement pulse evidencing pure shear on a planar fault. After discarding data with too shallow depth and from complex ruptures, 23 events were left for further study (Table 1).

On the basis of actual S/N spectral ratios, we selected a common upper cutoff frequency for analyzing all events and records, equal to 2.5 Hz. The lower cutoff for HF band was set at 0.5 Hz. When forming a set of records for a particular event, we applied the following rules:

1. the *S/N* ratio is no less than 2–3 at 2.5 Hz;
2. for each group of near stations that have recorded similar waveforms, only one is selected;
3. near-nodal records are rejected.

As a result, we keep from 5 to 18 records per station. These records are deconvolved for the channel transfer function and for the attenuation operator,

Table 1

Parameters of the earthquakes used for the study

No	Date	Time	Lat. °	Long.°	Depth, km	M_w	N_{sta}	Dur,s
1	1990/07/27	12:37:59	−15.35	167.46	125	7.2HRV	4	14
2	1993/01/15	11:06:05	43.30	143.69	102	7.6HRV	7	15
3	1993/05/24	23:51:28	23.23	−66.63	221	7.0NEIC	9	10
4	1993/08/09	12:42:48	36.37	70.86	214	7.0HRV	9	17
5	1994/02/11	21:17:31	−18.77	169.16	205	6.8HRV	10	8.0
6	1995/06/29	12:24:03	−19.54	169.28	139	6.6HRV	7	9.1
7	1995/10/21	02:38:57	16.84	−93.46	159	7.2HRV	10	25
8	1995/12/25	04:43:24	−6.90	129.15	141	7.1HRV	11	15
9	1996/04/16	00:30:54	−24.06	−177.03	110	7.2HRV	8	13
10	1997/05/03	16:46:02	−31.79	−179.38	108	6.9HRV	15	13
11	1997/09/02	12:13:22	3.85	−75.75	198	6.8HRV	9	10
12	1997/10/14	09:53:18	−22.10	−176.77	167	7.7HRV	9	20
13	1997/10/28	06:15:17	−4.36	−76.68	112	7.2HRV	8	16
14	1997/11/15	18:59:24	−15.14	167.37	123	7.0HRV	14	9.7
15	1998/01/04	06:11:58	−22.30	170.91	100	7.5HRV	6	25
16	1998/07/09	14:45:39	−30.48	−178.99	129	6.9HRV	12	11
17	1998/07/16	11:56:36	−11.04	166.16	110	7.0HRV	11	7.6
18	1998/12/27	00:38:26	−21.63	−176.37	144	6.8HRV	17	9.8
19	1999/02/06	21:47:59	−12.85	166.69	129	7.3HRV	10	11
20	1999/04/05	11:08:04	−5.59	149.57	150	7.4HRV	18	16
21	1999/05/10	20:33:02	−5.15	150.88	134	7.1HRV	19	9.8
22	2000/03/28	11:00:22	22.33	143.73	163	7.6HRV	18	15
23	2000/05/12	18:43:18	−23.54	−66.45	225	7.2HRV	10	14

N_{sta} – Number of records processed for each event; *Dur.* — duration of displacement pulse, average over stations.

with $t^* = 0.5$ (with phase correction). The result represents an initial velocity record. To form a well-defined displacement signal, the initial record is low-pass filtered with a zero-phase filter with 0.7 Hz upper cutoff, and then integrated, to produce an empirical estimate of $u(t)$, that we further denote as $m(t)$. The end of the displacement signal was selected as the moment of return to zero; when negative displacement was seen with amplitudes of up to $\approx$10% of initial motion, this part of the signal was substituted by zeros. If this part was more expressed, the record was rejected from analysis. To form the HF power signal, the initial record is filtered with a zero-phase band-pass filter; and the square of analytical signal is formed, giving an empirical estimate of $\dot{u}^2(t)$ that we denote as $p(t)$. Then we perform smoothing of $m(t)$ and $p(t)$, using the time window of boxcar shape, with the width Δt that is selected on a case by case basis, but typically about 0.8s; Δt is always a multiple of the initial time step 0.05 s. The results were decimated with the time step Δt, producing two sequences of statistically independent consecutive average amplitude values denoted as m_i, and p_i.

To determine $W_h(t)$ from observations, we first tried to average HF power signals of smaller, short-duration, intermediate-depth earthquakes $(M = 5.0–5.6)$, but ascertained that these records are too noisy to perform reliable averaging. We then took another approach and selected a number of records of earthquakes with $M = 5.8–6.2$, with relatively short durations of 2–3 s. Using (15) and approximating $W_o(t)$ with the displacement pulse, we selected, by trial and error, a credible approximation to $W_h(t)$, denoted $W_{h0}(t)$, common to all stations and earthquakes. Its analytical representation is (arbitrary scale):

$$W_{h0}(t) = 1000t \exp(-t/0.1) + [1.0t \exp(-t/1.5)]^{0.3}. \tag{16}$$

In discretized form, it reduces to a combination of a powerful delta-like spike and coda (Fig 1a). The shape (16) has been selected by trial and error on the basis of the analysis of about 50 records, at different stations, of eight earthquakes. On Figures 1bcd one can see that real HF pulses including codas are roughly comparable to predicted ones, though with occasional deviations. Artificial signal (16) was further applied to modify displacement records.

One might expect that the scattering effects in our case will be station-specific, because for intermediate-depth sources, scattering is localized mostly near a receiver. This being true, we might employ station-specific $W_h(t)$ functions. Data do not suggest such a sophistication however: the variations of relative P-coda amplitude between individual records at the same station seem to be of the same order of magnitude as between two stations. Thus, it seems reasonable to use the common shape like (16) in all cases.

During the main stage of the data processing, for each analyzed record, the following steps has been performed:
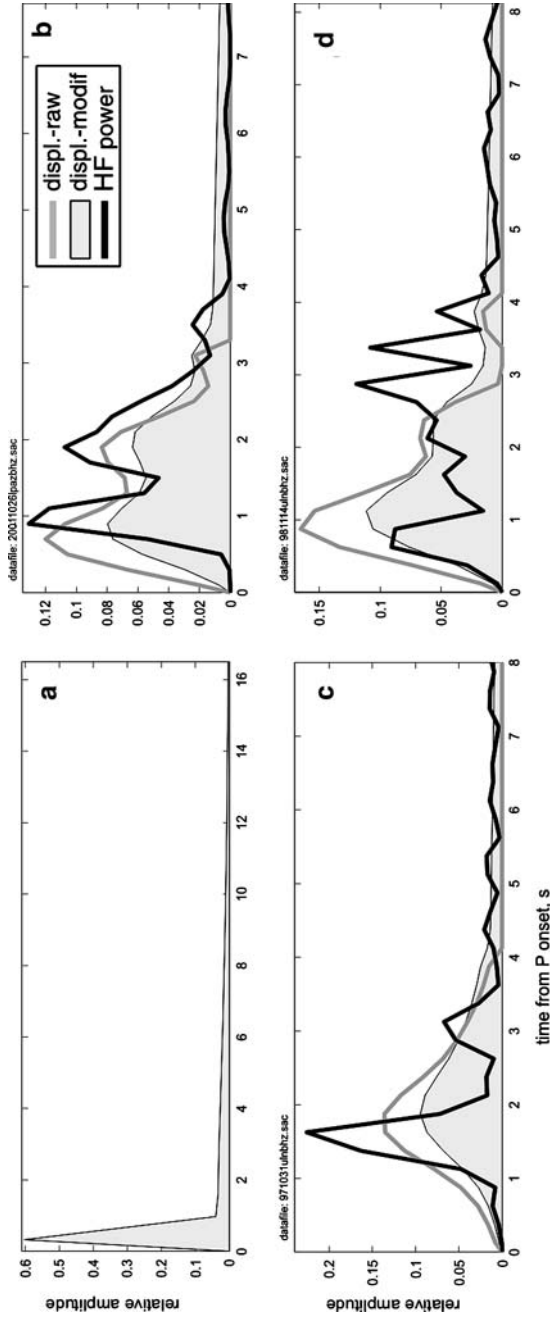
Figure 1

Examples of the performance of the selected standard HF power medium response (16). a—function (16) in discrete time scale; b, c, d—examples of application of the convolution procedure to discretized displacement records m_i of $M = 6$ earthquakes. Solid line: observed 0.5–2.5 Hz power signal p_i; gray line: observed displacement m_i; gray fill: modified displacement q_i, intended to emulate the coda part of HF power signal.

(1) Instrument and attenuation correction, band-pass filtering, and calculation of the HF power, resulting in two traces $m(t)$ and $p(t)$;

(2) selection of the onset time, common to $m(t)$ and $p(t)$, by visual inspection of both traces;

(3) selection of the end time for $m(t)$, using as criterion the return of the trace to the zero line;

(4) selection of the end time for $p(t)$, by visual inspection, either when the P-coda level becomes small or, fairly often, just before pP onset; and setting corresponding duration parameter d_m;

(5) convolution of $m(t)$ with the assumed $W_{h0}(t)$ (16) to obtain the modified displacement $q(t)$; setting the end time of $q(t)$ identical to that of $p(t)$, and determination of the common duration parameter d_p;

(6) using the preset common integer parameter $k_0 = 16$, determination of the time unit $\Delta t = \Delta t_0 (\text{Integer } (d_m/k_0) + 1)$, and the final number of time bins $k_1 = \text{Integer } (d_p /\Delta t)$ slicing the already isolated $m(t)$, $q(t)$ and $p(t)$ pulses in k, k_1 and k_1 identical time bins of duration Δt, and averaging each function over each bin; the resulting time sequences are denoted m_i, q_i and p_i;

(7) calculation of the correlation coefficients ρ_{ob} between q_i and p_i, (and also ρ_{ob0} between m_i and p_i over the first k segments, for comparison);

(8) determination of the estimates for $E(\rho_{idpr})$ and $\sigma(\rho_{idpr})$; this procedure includes: (a) generation of $N_{sim} = 25$ realizations of 0.5–2.5 Hz band-limited noise, (b) construction of 25 modulated HF signals $p_{sim}(t)$, using $q(t)$ as an envelope function; (c) application of step 6 to these signals, resulting in simulated sequences $p_{sim,i}$; (d) application of step 7 to pairs $(q_i, p_{sim,i})$ resulting in 25 "empirical" correlation coefficients $\rho_{idpr,i}$; (e) statistical analysis of this sample, that gives average $\rho_{idpr,av}$ and standard deviation s_{idpr}; these approximate $E(\rho_{idpr})$ and $\sigma(\rho_{idpr})$;

(9) calculation of the Student's t-value $(\rho_{idpr,av} - \rho_{ob})/s_{idpr}$ to judge the significance of the difference between ρ_{ob} and $\rho_{idpr,av}$.

In Figure 2 we show an illustration to Step 8. The variability of noise realizations is remarkable but still limited, and the actual observed $p(t)$ looks different from most of the noise realizations. The entire processing sequence is illustrated in Figure 3.

Results and their Analysis

To illustrate our processing procedure, in Table 2 we present the results for all analyzed records of a single event (No. 19 in Table 1). In Table 3 we compiled the aggregated results for all studied earthquakes. The analysis of these data can be summed up as follows.
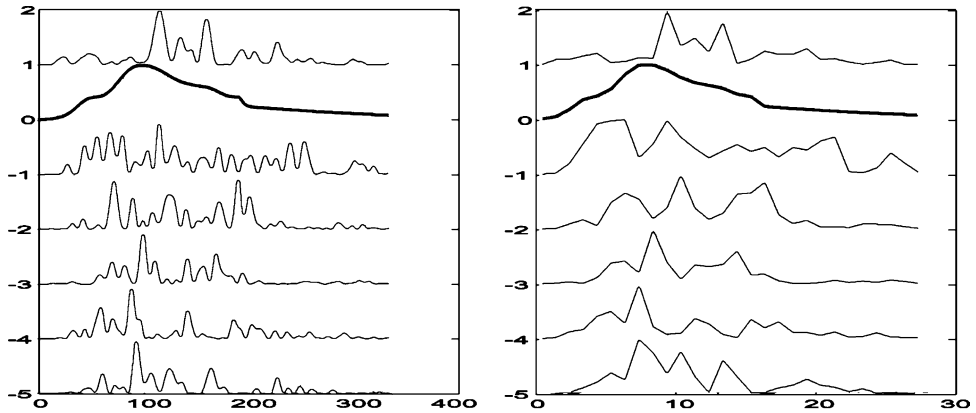
Figure 2

Illustration of the procedure used to estimate the significance of the displacement-HF power correlation. a: original HF power signals: "raw" HF power $p(t)$ signal (1), modified displacement $q(t)$ (2), and simulated HF power $p_{sim}(t)$ (five realizations 3–7), for the event 000328 at the station PFO. b: smoothed by 13 points and decimated variant of the same functions (denoted p_i; q_i; $p_{sim,i}$). All apparently significant variations of the data shown in a are preserved in b. The variability among the random realizations (3–7) is well-expressed, yet the actual observed signal (1) looks different from most of them, illustrating that the lack of tight correlation between (1) and (2) cannot be ascribed solely to the random fluctuations.

1. Source durations typically vary from 12 to 25 s, resulting in Δt values of 0.7–1.5 s. With $1/\Delta f \approx 0.5$ s, this gives a rather low number of degrees of freedom per single p_i (1.5–3). This means that p_i values must have a significant random scatter, and just this is seen on the simulations of Figure 2. For this reason, it is indeed critical to apply formal statistical analysis in order to determine whether the correlation between q_i and p_i is comparable or significantly lower than the similar correlation between q_i and $p_{sim,i}$.

2. The values of ρ_{ob} for individual records of a single earthquake vary significantly, but are systematically lower than $\rho_{idpr,av.}$, indicating the presence of genuine decorrelation. The standardized difference t (Student's value) varies significantly, and typically is around 2.3, giving significance levels between 20% (or more) and 0.1%, and typically about 5%. Since each record gives an independent observation, these probabilities from individual records of the same event must be multiplied to give the joint significance level. It is evidently very low, so that the statement "ρ_{ob} is below $\rho_{idpr,av}$" can be considered true even for the data set of a single earthquake. For the entire set of earthquakes, this conclusion can be considered as confidently proven.

3. The values of $\rho_{idpr,av}$ are rather stable, of the order of 0.7, and they indicate that "fluctuational" decorrelation is very significant. Thus the lack of close visual or formal correlation between $q(t)$ and $p(t)$ is guaranteed merely by the actual combination of the bandwidth and duration. On this background, "physical"
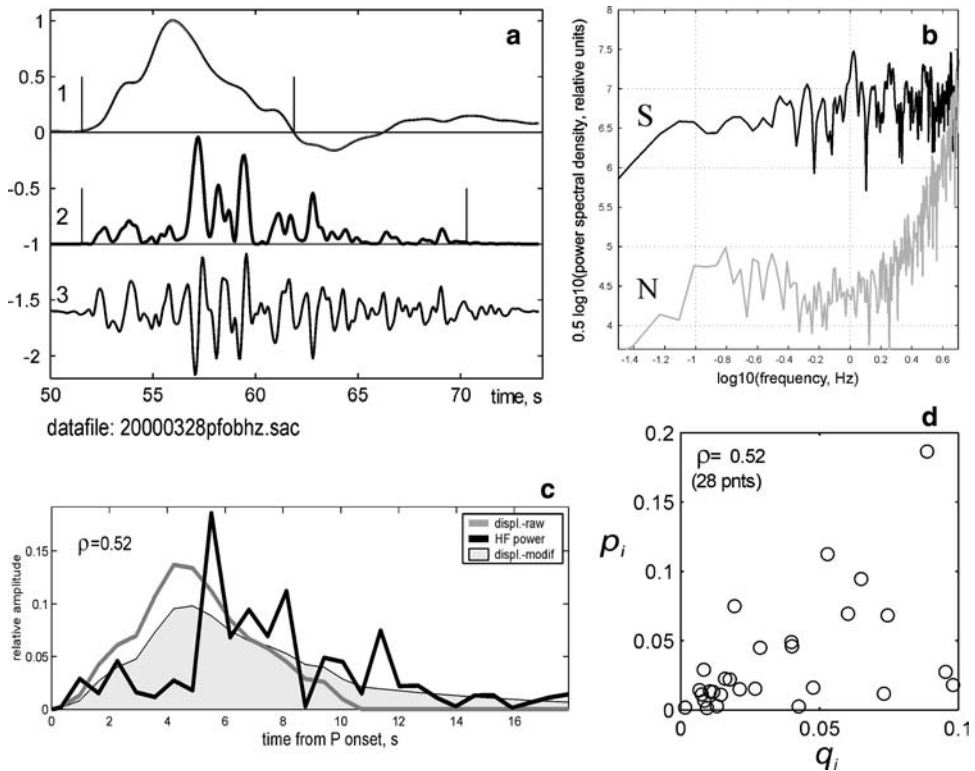
Figure 3

Processing procedure. a: selecting duration for displacement signal $m(t)$ (1) and HF power signal $p(t)$ (2); (3)—band-pass filtered velocity signal used to estimate (2). b: checking the S/N ratio using power spectra calculated for signal and for microseismic noise before P arrival. For this record S/N becomes low only above 4 Hz. c: obtained discretized raw m_i and modified q_i displacement signals, and "power" signal p_i; d: final correlation plot between q_i and p_i.

decorrelation, though present, in most cases is not visually clear, despite the cited definitive results of more formal statistical analysis.

4. Average values of ρ_{ob} for individual earthquakes fall into a relatively narrow range 0.35–0.65. The average over all earthquakes is 0.52.

In Figure 4 we show several m_i, q_i, and p_i sequences with various degrees of correlation. In some cases of low correlation, significant HF energy bursts occur near the end or even somewhat later than the visual end of a displacement pulse. On the average, there is a tendency of HF energy to be somewhat delayed with respect to displacement pulse. This tendency deserves deeper analysis.

To roughly estimate the ρ_{id} parameter, we apply the above-described procedure based on Equation (14). Departing from $E(\rho_{idpr}) = 0.72$ and $\rho_{ob} =$

Table 2

Parameters of individual records for the event 990206 (No. 19)

sta.	d_m,s	d_p, s	k_1	Δt, s	ρ_{ob0}	ρ_{ob}	ρ_{idprav}	s_{idpr}	t_{St}
anmo	14.6	17.3	18	0.95	0.14	0.32	0.74	0.092	−4.54
bjt	6.0	12.7	33	0.35	0.36	0.25	0.72	0.121	−3.82
brvk	15.3	15.6	16	0.95	0.02	0.24	0.64	0.156	−2.57
cola	10.5	15.7	23	0.65	−0.17	0.00	0.68	0.133	−5.12
ctao	10.4	13.0	19	0.65	0.07	0.35	0.64	0.090	−3.29
kurk	11.7	14.2	19	0.75	0.84	0.86	0.75	0.105	1.05
pfo	13.7	15.6	18	0.85	0.46	0.55	0.70	0.100	−1.51
tly	8.7	11.6	21	0.55	0.20	0.35	0.67	0.109	−2.96
uln	7.4	11.8	25	0.45	0.50	0.46	0.69	0.134	−1.69
yak	8.0	11.9	23	0.50	0.28	0.31	0.67	0.123	−2.92
average	10.6	13.9	22	0.66	0.27	0.37	0.69	0.116	−2.73
st.dev.	3.1	2.0	5	0.21	0.29	0.23	0.04	0.021	1.74

d_m and d_p : visually selected durations for the displacement pulse and for the 0.5–2.5 Hz power pulse; k_1: the number of time bins of size Δt within d_p ; Δt: the size of a time bin; ρ_{ob0} - correlation coefficient determined from m_i and p_i over the first k_0 = 16 bins (for reference only, further not used), ρ_{ob}: same, determined from q_i, and p_i over k_1 bins; ρ_{idprav} and s_{idpr}: average and standard deviation over 25 simulated $\rho_{idpr,i}$ values; t_{St} = (ρ_{ob} - ρ_{idprav})/ s_{idpr} – Student's *t*-statistic for testing the hypothesis ρ_{ob} < ρ_{idprav}.

0.52, we obtained the following estimates: z = 0.46, p = 0.57, and at last ρ_{id} = 0.80. Similarly, departing from the range of station averages for individual events ρ_{ob} = [0.35–0.65], we obtain the range for ρ_{id} values of individual events as [0.54–0.96]. These values represent our final results regarding "true" (ensemble-mean) values of the correlation coefficient between HF power and displacement signals.

Discussion

The average value of the correlation coefficient ρ_{ob} = 0.52 is the empirical average for a particular combination of source duration range and frequency band. The variations of ρ_{ob} between individual earthquakes, from 0.35 to 0.65, manifest real variations among earthquakes. The deviation of these values from unity has two components: random fluctuations of band-limited signal, and genuine difference between distributions of slip rate and mean luminosity. When the effect of fluctuations is excluded, the "ideal" average value ρ_{id} = 0.80 and the range 0.54–0.96 reflect intrinsic properties of the radiating faults ("physical decorrelation"). These values, when compared to $E(\rho_{idpr})$ = 0.72, mean that the fluctuational source of decorrelation is more powerful on the average, and that the degree of "physical decorrelation" is moderate. Both estimates (mean as well

Table 3

Average parameters (over stations) for each of the 23 earthquakes

No.	Event	ρ_{ob0} $\sigma\rho_{ob0}$	ρ_{ob} $\sigma\rho_{ob}$	ρ_{idprav} $\sigma\rho_{idprav}$	t_{St} $\sigma\, t_{St}$
1	900727	0.31	0.48	0.73	−2.94
		0.23	0.081	0.033	1.5
2	930115	0.37	0.51	0.75	−3.05
		0.31	0.21	0.058	2.8
3	930524	0.37	0.51	0.66	−1.54
		0.19	0.13	0.063	1.12
4	930809	0.28	0.42	0.74	−3.58
		0.20	0.23	0.048	2.7
5	940211	0.48	0.60	0.73	−1.4
		0.31	0.21	0.057	2.01
6	950629	0.35	0.41	0.72	−2.99
		0.22	0.24	0.062	2.9
7	951021	0.46	0.54	0.79	−3.3
		0.20	0.19	0.049	3.3
8	951225	0.52	0.62	0.75	−1.26
		0.22	0.17	0.066	1.9
9	960416	0.47	0.51	0.72	−1.76
		0.40	0.35	0.04	2.8
10	970503	0.47	0.35	0.70	−3.22
		0.34	0.29	0.069	2.7
11	970902	0.47	0.63	0.73	−1.07
		0.25	0.13	0.052	1.3
12	971014	0.49	0.56	0.77	−2.76
		0.22	0.28	0.079	2.7
13	971028	0.58	0.63	0.734	−0.98
		0.15	0.13	0.044	0.9
14	971115	0.44	0.54	0.74	−1.94
		0.28	0.22	0.032	2.2
15	980104	0.64	0.62	0.77	−1.49
		0.19	0.21	0.083	1.7
16	980709	0.39	0.48	0.71	−2.21
		0.26	0.27	0.055	2.1
17	980716	0.36	0.52	0.66	−1.11
		0.35	0.21	0.032	1.7
18	981227	0.38	0.46	0.67	−1.85
		0.35	0.24	0.068	2.4
19	990206	0.27	0.37	0.69	−2.74
		0.29	0.23	0.038	1.7
20	990405	0.39	0.46	0.75	−3.69
		0.20	0.15	0.050	2.5
21	990510	0.57	0.56	0.70	−1.28
		0.24	0.27	0.038	2.4

as the range) can be treated as describing the decorrelation between, respectively, individual and mean distributions of the slip rate and mean luminosity over the fault surface.

Table 3

(*contd.*)

No.	Event	ρ_{ob0} $\sigma\rho_{ob0}$	ρ_{ob} $\sigma\rho_{ob}$	ρ_{idprav} $\sigma\rho_{idprav}$	t_{St} $\sigma\, t_{St}$
22	000328	0.31	0.50	0.68	−1.84
		0.36	0.30	0.053	3.2
23	000512	0.48	0.55	0.72	−1.55
		0.27	0.25	0.025	2.1
	average	0.427	0.52	0.72	−2.16
	st.dev.1	0.096	0.079	0.036	0.88
	st.dev.2	0.26	0.22	0.052	2.23

For each earthquake, the four values ρ_{ob0}, ρ_{ob}, ρ_{idprav}, and t_{St} are averages over individual stations processed, (as illustrated by the last but one line of Table 2). In the main part of the table, two lines are given for each earthquake: the upper one contains mean values over N_{sta} records, and the lower one, italicized, contains standard deviations obtained in averaging over several records of the same earthquake. The three bottom lines contain: *average* over events (i.e., over station averages), standard deviation *st.dev.1* among events, and *st.dev.2* – the average over "within-event" standard deviations, respectively.

Conclusions

1. Having analyzed 251 teleseismic records of 23 intermediate-depth earthquakes, we found that the correlation between time histories of displacement and of HF (0.5–2.5Hz) squared velocity is limited, with the average correlation coefficient equal to 0.52; the range of averages over the multiple records of an individual earthquake varies from 0.35 to 0.65.
2. There are two causes of the decorrelation between displacement and HF squared velocity signals: (1) inevitable fluctuations of noise-like HF signal, and (2) genuine mismatch between displacement signal and mean-square envelope of HF signal. Acting separately, these factors would result in the following values of correlation coefficient: fluctuation-related: 0.72 (average); genuine: 0.80 (average), 0.54 to 0.96 (the range for individual earthquakes).
3. Our estimates of correlation coefficient between displacement and high-frequency (HF) squared amplitude of *P*-wave signal can be treated as upper bound estimates for the correlation coefficient between local source slip rate and local HF *P*-wave luminosity (or radiated HF power flux) for the same spot of the fault.
4. The above results can be used as an initial approximation to constrain realistic simulation of earthquake sources; they may also be applied to verify advanced dynamic models of an earthquake fault.
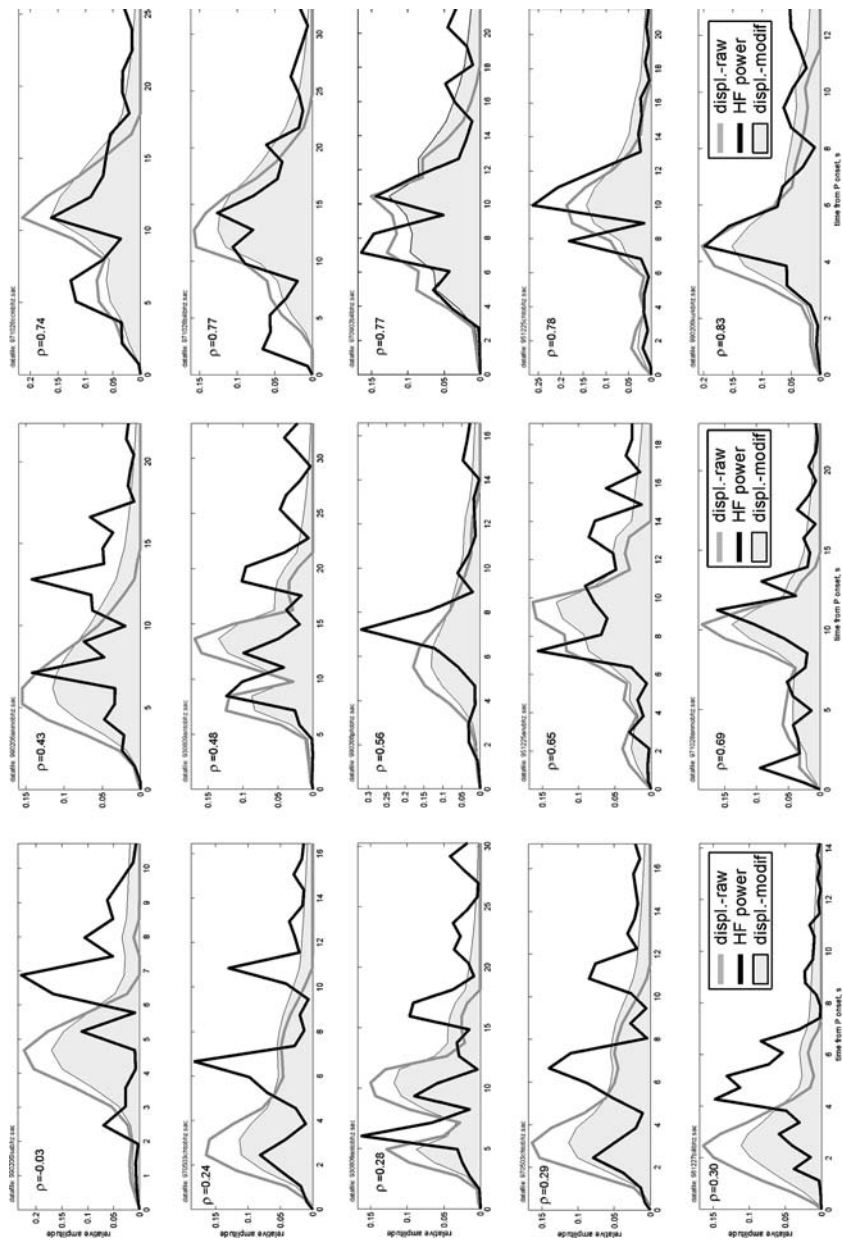
Figure 4

Examples of various degrees of correlation between HF power p_i and modified displacement q_i, ordered according to the value of ρ_{ob}. In the upper left edge of each frame, a file name is given, of the form yymmddsssbhz.sac where yymmdd is the date of event and sss is the station name.

Acknowlegements

Fruitful discussions with Victor Pavlov and Fabio Romanelli are here acknowledged. We appreciate valuable suggestions of the editor K. Kuge and an anonymous reviewer that improved the manuscript. This work is a contribution to the Italian MIUR-COFINANZIAMENTO projects 2001045878_007 and 2002047575_002.

REFERENCES

AKI, K. (1967), *Scaling law of seismic spectrum,* J. Geophys. Res. *72*, 1217–1231.

ANDREWS, D.J. (1980), *A stochastic fault model. I. Static case,* J. Geophys. Res. *85*, 3867–3877.

BLANDFORD, R.R. (1975), *A source theory for complex earthquakes,* Bull. Seismol. Soc. Am. *65*, 1385–1405.

BOATWRIGHT, J. (1982), *A dynamic model for far-field acceleration,* Bull. Seismol. Soc. Am. *72*, 1049–1068.

BOATWRIGHT, J. (1988), *The seismic radiation from composite models of faulting,* Bull. Seismol. Soc. Am. *78*, 489–508.

GUSEV, A.A. (1983), *Descriptive statistical model of earthquake source radiation and its application to an estimation of short-period strong ground motion,* Geophys. J. R. Astron. Soc. *74*, 787–800.

GUSEV, A.A. (1989), *Multiasperity fault model and the nature of short-period subsources,* Pure Appl. Geophys. *130*, 635–660.

GUSEV, A.A. and PAVLOV, V.M. (1991), *Deconvolution of squared velocity waveform as applied to study of non-coherent short-period radiator in earthquake source,* Pure Appl. Geophys. *136*, 236–244.

GUSEV, A.A. and PAVLOV, V.M. (1998), *Preliminary determination of parameters of the high-frequency source for the Dec. 05, 1997 Mw = 7.9 Kronotsky earthquake.* In *XXVI Gen. Assembly,* Eur. Seismol. Commission, Papers, Tel-Aviv, Israel, pp. 73–77.

IIDA, M. and HAKUNO, M. (1984), *The difference in the complexities between the 1978 Miyagiken-oki earthquake and the 1968 Tokachi-oki earthquake from a viewpoint of the short-period range,* Natural Disaster Sci. *6*, 1–26.

ISHIMARU , A., *Wave Propagation and Scattering in Random Media, vols. 1 and 2* (Academic, San Diego, California 1978).

HANKS, T.C. (1979), *b values and ω⁻ʸ seismic source models: Implication for tectonic stress variations along active crustal fault zones and the estimation of high-frequency strong ground motion,* J. Geophys. Res. *84*, 2235–2242.

KAKEHI, Y. and IRIKURA, K. (1996), *Estimation of high frequency wave radiation areas on the fault plane by the envelope inversion of acceleration seismograms,* Geophys. J. Int. *125*, 892–900.

NISHIMURA, T., NAKAHARA, H., SATO, H., and OHTAKE, M. (1996), *Source process of the 1994 far east off Sanriku earthquake, Japan, as inferred from a broad-band seismogram,* Sci. Rep. Tohoku Univ. *34*, 121–134.

PAPAGEORGIOU, A.S. and AKI, K. (1983), *A specific barrier model for the quantitative description of inhomogeneous faulting and the prediction of strong ground motion. Part I: Description of the model,* Bull. Seismol. Soc. Am. *73*, 693–722.

PETUKHIN, A.G., NAKAHARA, H., and GUSEV, A.A. (2004), *Inversion of the high-frequency source radiation of M6.8 Avachinsky Gulf, Kamchatka, earthquake using empirical and theoretical envelope Green functions,* Earth Planets Space *56*, 921–925.

ZENG, Y., AKI, K., and TENG, T.-L. (1993), *Mapping of the high frequency source radiation for the 1989 Loma Prieta Earthquake, California,* J. Geophys Res. *98*, 11,981–11,993.

To access this journal online:
http://www.birkhauser.ch